# Applications of the polarizability model to various displacive-type ferroelectric systems

A. Bussmann-Holder
*Universität Bayreuth and Max-Planck-Institut für Festkörperforschung, Heisenbergstrasse 1, 7000 Stuttgart 80, Federal Republic of Germany*

H. Bilz*
*Max-Planck-Institut für Festkörperforschung, Heisenbergstrasse 1, 7000 Stuttgart 80, Federal Republic of Germany*

G. Benedek
*Dipartimento di Fisica dell'Università and Gruppo Nationale di Struttura della Materia del Consiglio Nazionale delle Ricerche, Via Celoria 16, 20133 Milano, Italy*
(Received 28 November 1988)

We apply the theory of ferroelectricity in the framework of the polarizability model, which has been presented in a previous paper, to various classes of displacive-type ferroelectrics. We show that the experimental data of temperature-dependent quantities like soft-mode frequencies and dielectric constants can be well reproduced using a very limited set of parameters. We present results for $ABO_3$ perovskites, IV-VI compounds, SbSI, $K_2SeO_4$, hydrogen-bonded ferroelectrics, antiferroelectric compounds, and their mixed isostructural ferroelectrics.

## INTRODUCTION

In a previous paper a polarizability model was introduced to describe the dynamical properties of displacive-type ferroelectric compounds.[1] The model is based on the anisotropic nonlinear polarizability of the oxygen ion and its homologues[2] which dynamically has been taken into account in terms of a local double-well potential.[3] The application of the self-consistent phonon approximation (SPA) to the nonlinear problem allows the calculation of temperature-dependent quantities as, e.g., dispersion curves, soft-mode frequencies, dielectric constants, and related quantities. As the model is pseudo-one-dimensional considering only the ferroelectric direction,[4] the few model parameters exhibit real physical meanings, and changes caused by applications to various systems can directly be related to the intrinsic properties of the system under consideration. In this paper we want to show the variety of applications of the polarizability model which has been treated theoretically in the previous paper (hereafter called I). We will show that independent of structural differences, the model is applicable to displacive-type ferroelectrics, as only the ferroelectric direction is relevant from the lattice dynamical point of view. We rediscover the different temperature regimes predicted in a previous paper[5] and compare it to experimental results.

## I. PEROVSKITES $ABO_3$

The ferroelectric properties of perovskites ($ABO_3$) were first discovered for $BaTiO_3$ by Wul and Goldman.[6] Shortly thereafter, the whole class of perovskites as well as their ceramics and alloys were discovered by several people, i.e., Matthias,[7] Matthias and Remeika,[8] and Shirane *et al.*[9] Because of their high stability, good growing conditions, and high dielectric anomalies, the applications of $ABO_3$ compounds are many. At the same time, the very simple structure of $ABO_3$ compounds is a challenging tool for theoretical investigations. As initially pointed out by Cochran,[10] and discussed previously,[1] the perovskite structure has some features in common with the cubic CsCl structure. Therefore, the reduction from a three-dimensional lattice to one that is pseudo-one-dimensional could easily be accomplished. Within the simple model we investigated three perovskite-type crystals, two of which are incipient ferroelectrics $SrTiO_3$ and $KTaO_3$, and one with a classical soft-mode behavior and high $T_c$, $PbTiO_3$. For all three compounds the lowest transverse acoustic mode and the lowest transverse optic mode have been calculated as a function of $q$ for the ferroelectric axis. The temperature dependence of the soft-mode frequency $\omega_F$ was calculated self-consistently. While for $SrTiO_3$ and $KTaO_3$ a rigid cationic sublattice was assumed, i.e., $g_2^{(2)}=0^1$, in $PbTiO_3$ the lead polarizability had to be included in the calculations. Simultaneously the cationic core-core coupling $f'_{(2)}$ entered the procedure (see paper I).

As can be seen in Fig. 1, good agreement could be achieved between calculated and experimental[11–13] dispersion curves.

For $SrTiO_3$, the TO modes lying in between have not been taken into account in the calculation because of reasons of symmetry. The dispersion curves of $PbTiO_3$ exhibit, at small $q$ values, an interesting peculiarity which is also observed in other ferroelectric systems. The experimentally observed TA-phonon anomaly close to $\frac{2}{3}$ of the Brillouin-zone edge can be reproduced theoretically by including the coupling of nonlinear solutions of the equations of motion to SPA phonons in the calculations which have been discussed in Ref. 14. The temperature

 

dependence of the squared soft-mode frequency is shown in Fig. 2. Again, nearly perfect agreement between experiment and theory could be achieved. Close to $T_c$, $T=0$, all three compounds display, in their soft mode-frequency, deviations from mean-field behavior, i.e., $\omega^2 \approx (T-T_c)^{\gamma}$, $\gamma=1$. In $SrTiO_3$ and $KTaO_3$ these deviations are well understood because of the enhancement of dimensionality due to quantum fluctuations.[15] In $PbTiO_3$ the first-order nature of the phase transition is responsible for the observed discrepancy.

The model parameters of the three compounds are listed in Table I. Due to the same anionic cluster, $f$ and $f'_{(1)}$

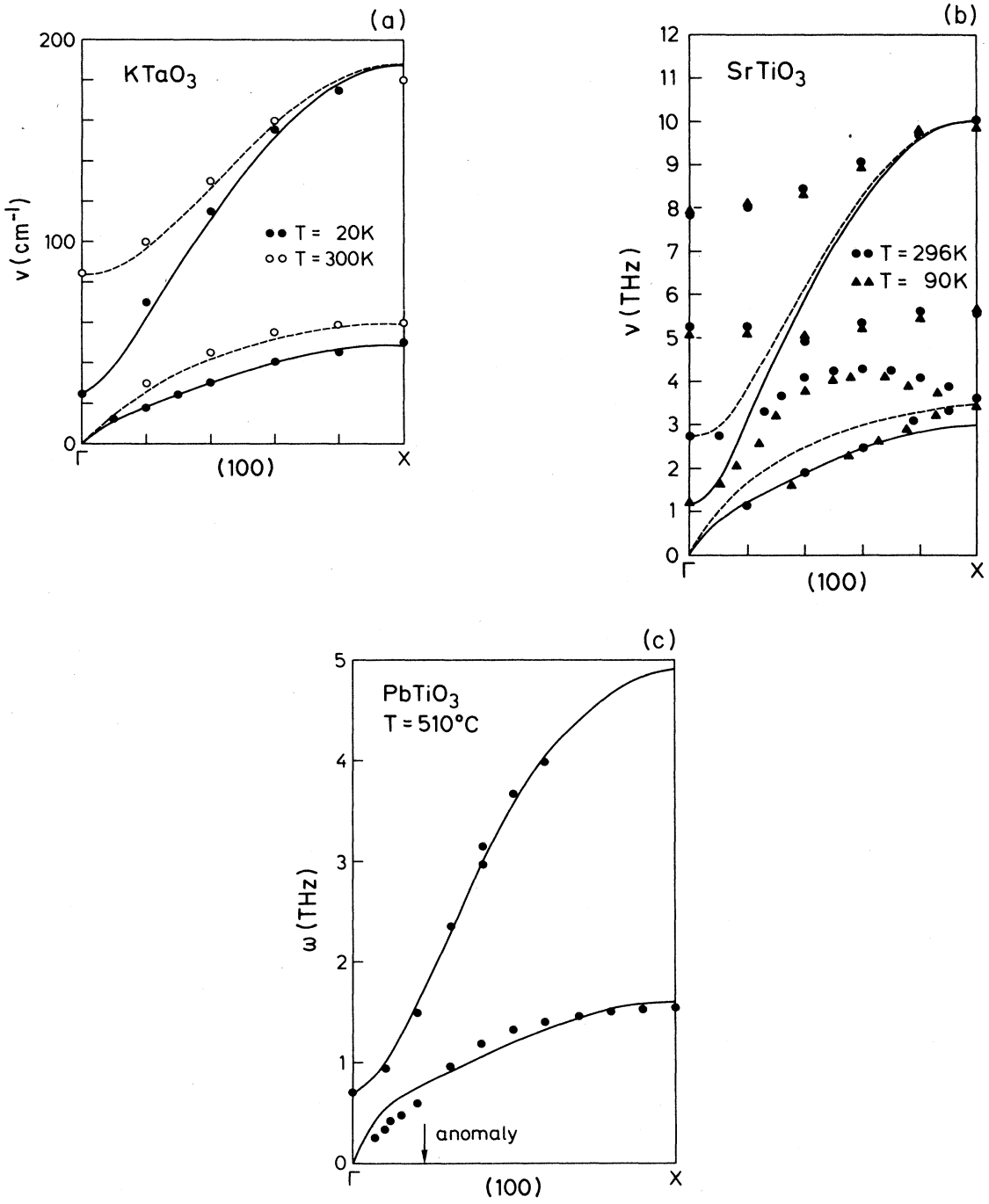


FIG. 1. Comparison of experimental and theoretical dispersion curves for (a) $KTaO_3$ at 20 K (straight line, solid circles) and at 300 K (dashed line, open circles). Experimental data (circles) have been taken from Ref. 11; (b) $SrTiO_3$ at 90 K (straight line, triangles) and at 296 K (dashed line, full circles). Experimental data (circles and triangles) have been taken from Ref. 12; (c) $PbTiO_3$ at 510 °C (straight line: theory; circles: experiment Ref. 13).

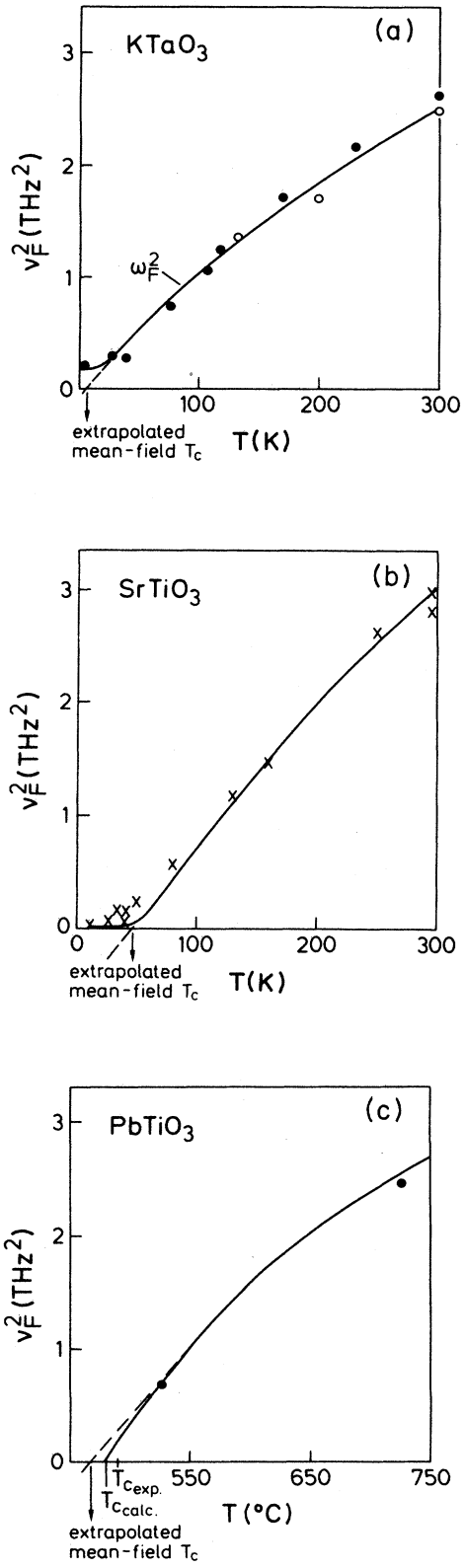


FIG. 2. Comparison of experimental [circles (Ref. 11), crosses (Ref. 12), and triangles (Ref. 13)] and theoretical temperature dependences of $\omega_F^2$ for (a) $KTaO_3$, (b) $SrTiO_3$, (c) $PbTiO_3$.

are of the same order of magnitude for $SrTiO_3$ and $PbTiO_3$. The instability of the system under consideration is mainly determined by $g_2^{(1)}$. As can be seen from the table, $|g_2^{(1)}|$ increases when going from $KTaO_3$ via $SrTiO_3$ to $PbTiO_3$, thus indicating the increasing softness and also the increase in $T_c$.

## II. IV-VI SEMICONDUCTORS

The IV-VI compounds have ten electrons per unit cell as do the group V elements and the III-VII compounds. All of these systems crystallize either in the rock-salt structure characteristic of ionic compounds, or in a distorted rock-salt structure where covalent bonds can be formed.[16] GeTe and SnTe become ferroelectric at $T_c=670$ K and $T_c=98$ K,[17] respectively. Their low-temperature rhombohedral structure can be obtained from the NaCl structure by displacing the two sublattices relative to each other along the $\langle 111 \rangle$ axis and by stretching the unit cell along this axis.[18] The nonferroelectric rock-salt structure compounds PbS, PbSe, and PbTe can be transformed into a rhombohedral structure by hydrostatic pressure.[19] As has been shown for perovskites, the layer-type model works well for the so-called diagonally cubic direction, which in IV-VI compounds is equivalent to the $\langle 111 \rangle$ direction.[20] As before, the lowest TA and TO modes have been calculated for SnTe, PbTe, PbSe, and PbS. The temperature dependence of $\omega_F^2$ has been calculated for SnTe and PbTe, while for the two other compounds no experimental data are available.

The model parameters $g^{(1)}$, $g^{(2)}$, $f$, $f'_{(1)}$, and $f'_{(2)}$ have been determined by fitting the theoretical data to the experimental curves. The nonlinearly polarizable sublattice with mass $m_1$ is given by the chalcogenide ion mass while $m_2$ was given by Sn or Pb. Figure 3 shows the experimental dispersion curves for PbS,[21] PbSe,[22] PbTe,[23] and SnTe (Ref. 24) compared to the calculated curves. Starting with the parameter set of PbS, the substitution of sulfur by another chalcogenide ion mass mainly lowers the frequencies of the transverse optic mode at the zone center and the zone boundary. Additional slight adjustments of the model parameters lead to the resulting theoretical curve. The model parameters of the lead chalcogenides and SnTe are listed in Table II. For all compounds the second-nearest-neighbor core-core coupling constants $f'_{(1)}$ and $f'_{(2)}$ are of the same order of magnitude. As the cationic polarizability is rather small,

TABLE I. Model parameters of $ABO_3$ ferroelectrics.

| | $SrTiO_3$ | $KTaO_3$ | $PbTiO_3$ |
|---|---|---|---|
| $m_1$ ($10^{-22}$ g) | 1.549 | 2.88 | 1.65 |
| $m_2$ ($10^{-22}$ g) | 1.461 | 0.649 | 3.44 |
| $f$ ($10^4$ g s$^{-2}$) | 14.405 | 4.067 | 13.00 |
| $f'_{(1)}$ ($10^4$ g s$^{-2}$) | 1.268 | 0.581 | 0.912 |
| $f'_{(2)}$ ($10^4$ g s$^{-2}$) | | | 17.27 |
| $g^{(2)}$ ($10^4$ g s$^{-2}$) | | | 28 |
| $g_2^{(1)}$ ($10^4$ g s$^{-2}$) | −2.629 | −0.828 | −5.171 |
| $g_4$ ($10^{22}$ g s$^{-2}$ cm$^2$) | 0.904 | 0.255 | 4.606 |

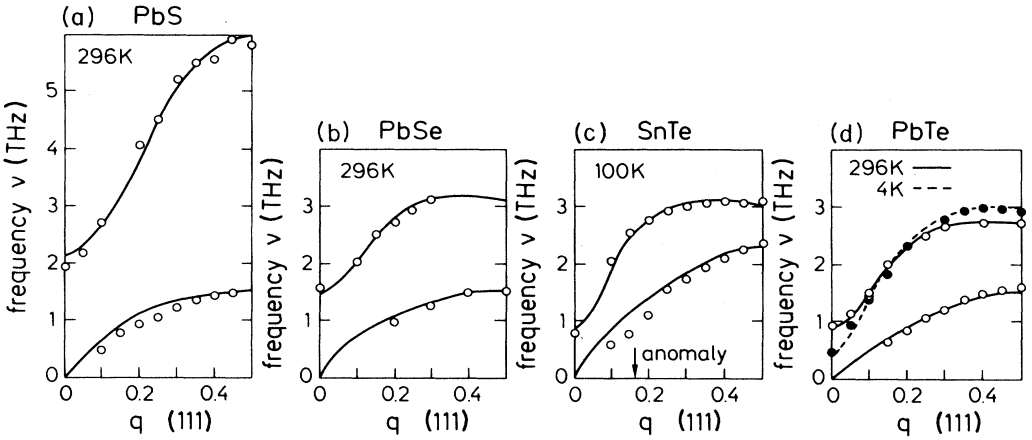


FIG. 3. Comparison of calculated dispersion curves (lines) with the experimental data (dots) for (a) PbS (Ref. 21), (b) PbSe (Ref. 22), (c) SnTe (Ref. 24), and (d) PbTe (Ref. 23).

the core-shell coupling constant $g^{(2)}$ has large values, which is the same for all compounds. The main parameter changes come up in the next-nearest-neighbor coupling $f$ and the temperature-dependent anionic polarizability $g^{(1)}(T)$. The increase in $f$ with increasing cationic mass is a consequence of the more and more repulsive forces between neighboring atoms, i.e., the growing overlap between anion and cation. As has been pointed out before for perovskites, $g^{(1)}(T)$ is a measure of the "softness" of the system under consideration. Consequently the anionic core-shell coupling decreases when going from PbS to PbTe and exhibits the lowest value for SnTe which undergoes a ferroelectric transition. Again, it should be noted that the experimentally observed TA mode of SnTe exhibits a dip at $qa \cong \pi/3$ which cannot be reproduced by the simple model. A possible explanation of this phonon anomaly has been given in another paper.[25] The temperature dependence of the soft mode in the paraelectric phase has been calculated for PbTe (Ref. 26) and SnTe,[24] and for SnTe the ordinary and extraordinary modes[27] of the ferroelectric phase could be calculated too.

Figure 4 shows the temperature dependence of $\omega_F^2$ for PbTe. Again, deviations from a mean-field behavior, i.e., $\gamma = 1$, can be observed. It is interesting to note that as an outcome of the SPA, PbTe will never become a ferroelectric, as its harmonic electron-phonon-coupling term $g_2^{(1)}$ is repulsive, i.e., it does not exhibit a harmonic instability. The temperature dependence of $\omega_F^2$ of SnTe in the paraelectric and the ferroelectric phases is depicted in Fig. 5. Very close to $T_c$ deviations from mean-field behavior occur which lead to a $T_c$ of 98 K instead of the mean-field extrapolated $T_c$ of 79 K. Because of the cubic structure in the paraelectric phase of SnTe, two transverse soft modes are degenerate. This degeneracy is lifted in the low-temperature tetragonal phase which consequently leads to the observation of two soft modes. Within the model, the mode splitting has been taken into account by a weighting factor of 3 for the extraordinary (EO) mode, i.e., $g_{2EO}^{(1)} = 3g_{2O}^{(1)}$ (O denotes ordinary), and $g_{4EO}^{(1)} = 3g_{4O}^{(1)}$, respectively. As can be seen, good agreement between experiment and theory could be achieved by this procedure.

TABLE II. Model parameters.

| | PbS | PbSe | PbTe | SnTe |
|---|---|---|---|---|
| $f'_{(1)}$ ($10^4$ g s$^{-2}$) | 1.65 | 0.55 | 0.75 | 0.98 |
| $f'_{(2)}$ ($10^4$ g s$^{-2}$) | −1.00 | −2.00 | −1.80 | −2.20 |
| $g^{(1)}$ ($10^4$ g s$^{-2}$) | 0.95 | 0.85 | 0.45 | 0.30 |
| $g^{(2)}$ ($10^4$ g s$^{-2}$) | 28.00 | 28.00 | 28.00 | 28.00 |
| $f$ ($10^4$ g s$^{-2}$) | 4.50 | 12.00 | 13.00 | 18.50 |
| $m_1$ ($10^{-22}$ g) | 0.53 | 1.31 | 2.12 | 2.12 |
| $m_2$ ($10^{-22}$ g) | 3.44 | 3.44 | 3.44 | 1.97 |

## III. SbSI

The crystals of SbS$J$ belong to the family of V-VI-VII compounds (where V=Sb, Bi; VI=S, Se, and Te; VII=Cl, Br, and I) which crystallize in an orthorhombic structure.[28] Their unusual photoelectric properties have

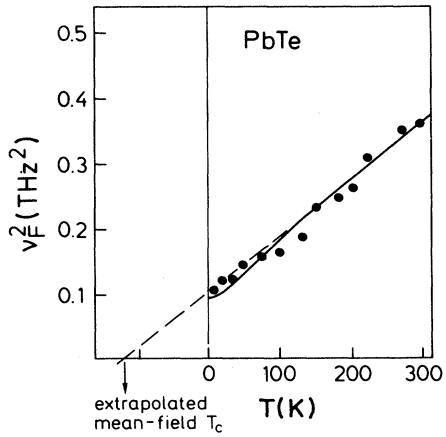


FIG. 4. Comparison of experimental (circles) and theoretical (line) temperature dependence of $\omega_F^2$ for PbTe.

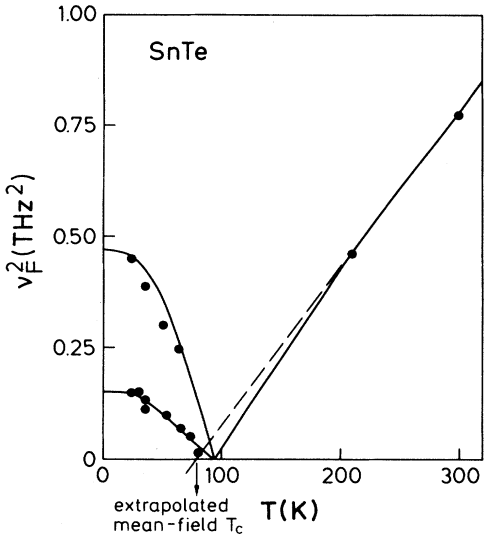


FIG. 5. Comparison of experimental (circles) and theoretical (lines) temperature dependences of $\omega_F^2$ for SnTe in the paraelectric (Ref. 24) and the ferroelectric phase (Ref. 27).

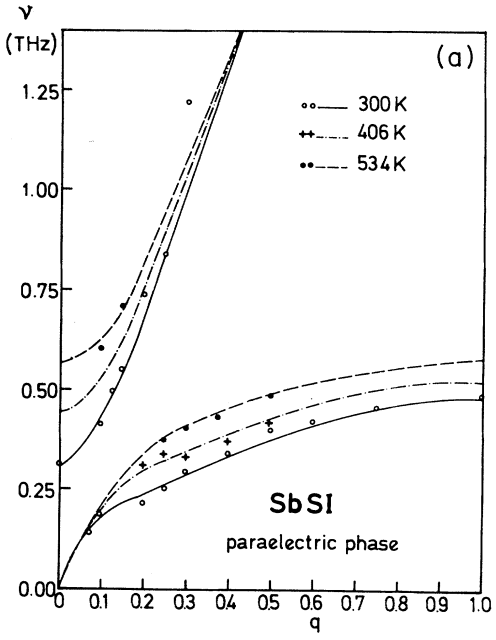


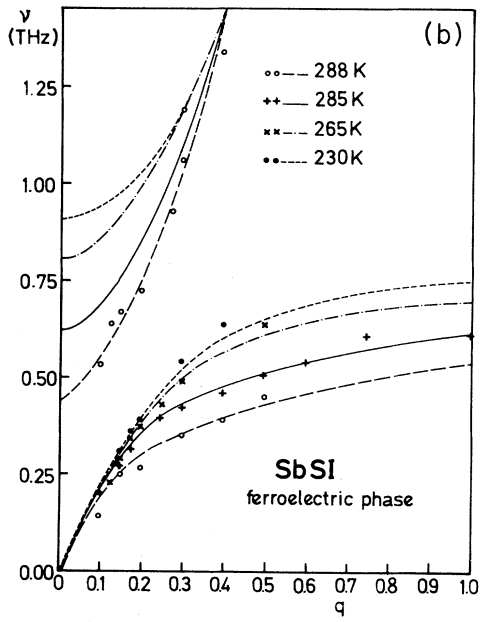


FIG. 6. Comparison of calculated dispersion curves (lines) with experimental data (Ref. 32) at different temperatures for SbS*J* in (a) the paraelectric phase, and (b) the ferroelectric phase.

attracted theoretical[29] and experimental research as well.[30] Ferroelectricity was first discovered in SbSI which undergoes a phase transition at room temperature.[29] Later, also other members of this family were found to become ferroelectric, but at much lower temperatures.[31] The crystals of SbSI show a needlelike shape; the ferroelectric axis is the needle ($c$) axis.[28] Their spontaneous polarization, the static dielectric constant, and the Curie constant are of the same order of magnitude as of classical perovskite-type ferroelectrics ($BaTiO_3$, $KNbO_3$, $PbTiO_3$). The application of a diatomic model to SbS*J* can be made possible by taking the SbS complex as the highly polarizable sublattice (equivalent to the perovskite $BO_3$ unit), while the halogenide ions are assumed to be rigid and equivalent to the perovskite $A$ cations.

For SbS*J*, measurements of the lowest TA and TO mode have been carried out in the paraelectric and the ferroelectric regimes as well.[32] The experimental points and theoretical dispersion curves are compared to each other in Figs. 6. The parameters $f$ and $f'_{(1)}$ have been kept constant for both phases, while $g_2^{(1)}$ and $g_4^{(1)}$ change sign and value when passing through $T_c$. A striking feature in the TA-phonon dispersion is again, as in SnTe and $PbTiO_3$, the dip close to $qa \cong \frac{1}{3}$. The variation of $\omega_F^2$ with temperature[33] is shown in Fig. 7.

According to the model predictions, $\omega_F^2$ saturates at high temperatures with a critical exponent $\gamma$ close to $\frac{1}{3}$. As in the ferroelectric phase, the soft mode crosses with temperature-independent modes[34] the calculation of $\omega_F^2(T)$ could not be carried out for this phase. The model parameters used are listed in Table III. The high absolute value of $g_2^{(1)}$ (similar to $PbTiO_3$) again reflects the softness and high $T_c$ of SbS*J*.

## IV. $K_2SeO_4$

The phase transitions of $K_2SeO_4$ have been discussed in more detail in Ref. 14. Here, we concentrate only on the results of the SPA, which, in this case, are by no means sufficient to explain the experimentally observed phenomena. $K_2SeO_4$ undergoes two successive phase transitions from an orthohombic paraelectric phase to an incommensurate phase at $T_i = 130$ K. At 93 K the structure

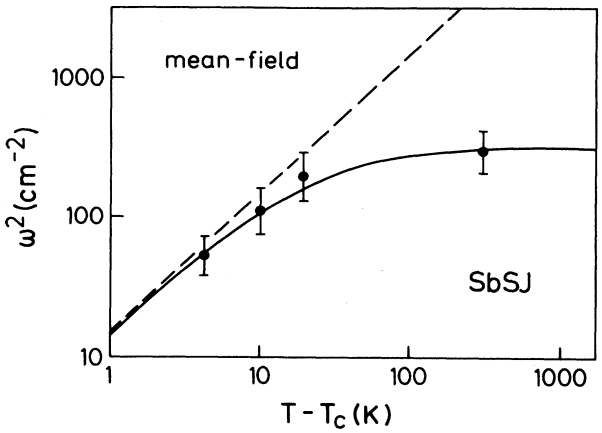


FIG. 7. Comparison of experimental (Ref. 33) (circles) and theoretical temperature dependence of $\omega_F^2$ for SbSJ.

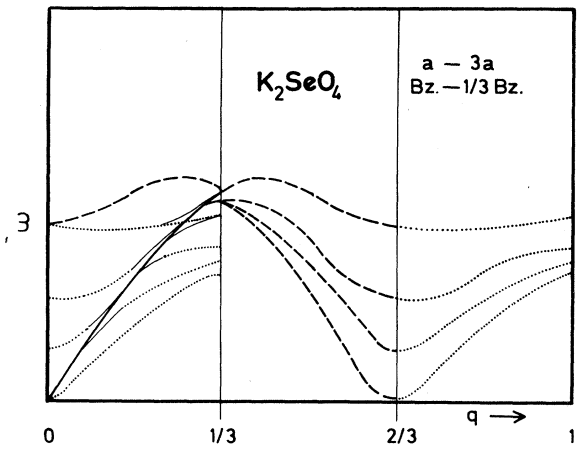


FIG. 8. Dispersion of the transverse acoustic branch of $K_2SeO_4$ and the reduction of the Brillouin zone to $\frac{1}{3}$.

becomes commensurate ferroelectric.[35,36] The first transition is accompanied by the softening of the TA branch close to $qa \cong (2\pi/3,0,0)$. The lock-in transition at 93 K is characterized by a tripling of the unit cell.[37] The pseudo-threefold symmetry which reveals itself in the $a,b$ plane and explains the occurrence of a soft mode at $qa=(2\pi/3,0,0)$ can be explained crystallographically, if, according to the notation of Kalman *et al.*,[38] the two symmetrically nonequivalent potassium ions $K_\alpha$ and $K_\beta$ and the $SeO_4$ complex are taken to be equivalent. A reduction of the $K_2SeO_4$ unit cell to a CsCl-type structure is possible by assuming that the $K_\beta$ ions are negligible, while the $K_\alpha$ ions have twice the mass of the potassium ion. By means of this simplification it is possible to apply the pseudo-one-dimensional model to $K_2SeO_4$. As within the SPA, it is only possible to calculate the temperature dependence of the $q=0$ soft phonon; the Brillouin zone of $K_2SeO_4$ is folded back twice and the incommensurate deviations from $2\pi/3$ are neglected (Fig. 8). The results of the model calculations are compared to experimental data in Fig. 9. The temperature dependence of the "pseudo $q=0$" soft mode has been calculated self-consistently for the paraelectric and the ferroelectric regimes. Interestingly, the soft mode shows an anomaly at the incommensurate transition temperature $T_i$, but definitely softens at $T_c$. Below $T_c$, "normal" ferroelectric behavior is observed (Fig. 10). It is interesting to note that within the simple layer model the harmonic electron-phonon coupling is repulsive in the paraelectric state, while $g_4$ is attractive. Both $g_2^{(1)}$ and $g_4$ change sign in the incommensurate phase and once again in the ferroelectric regime. Thus, only the ferroelectric phase exhibits the "normal" behavior of these local quantities.

As mentioned earlier, the previously described treatment of the phase transitions of $K_2SeO_4$ is not sufficient to reproduce the experimentally observed features. Yet by assuming the described simplifications it is possible to explain the soft-mode behavior of $K_2SeO_4$.

TABLE III. Model parameters of SbSJ.

| | |
|---|---|
| $m_1$ ($10^{-22}$ g) | 2.556 |
| $m_2$ ($10^{-22}$ g) | 2.107 |
| $f$ ($10^4$ g s$^{-2}$) | 2.066 |
| $f'_{(1)}$ ($10^4$ g s$^{-2}$) | 0.048 |
| $g_2$ ($10^4$ g s$^{-2}$) | −10.994 |
| $g_4$ ($10^{22}$ g s$^{-2}$ cm$^{-2}$) | 0.056 |

## V. HYDROGEN-BONDED CRYSTALS

The lattice dynamics of hydrogen-bonded crystals are exemplified for $KH_2PO_4$ and its isomorphic compounds. The outstanding properties of these ferroelectrics is the large isotope effect on $T_c$ and the Curie constant upon deuteration.[39] The most widely accepted theoretical model is the coupled-proton lattice model including proton tunneling,[40] which by the use of new experimental techniques[41] exhibits obvious failures. In a recent review on these compounds, the conclusion was drawn that new theories are needed to explain the observed phenomena.[42] As in the above described ferroelectrics, only one crystal-

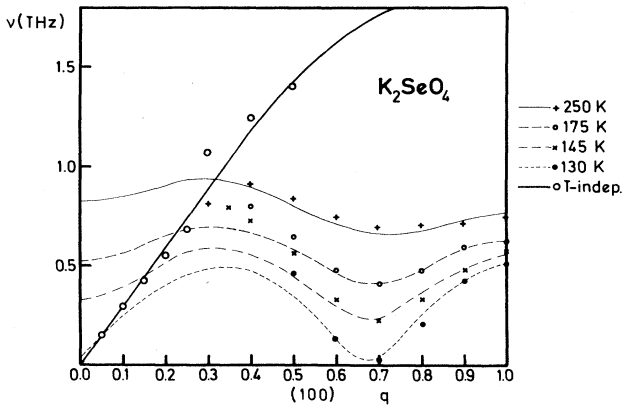


FIG. 9. Comparison of theoretical (lines) with experimental (Ref. 37) dispersion curves for $K_2SeO_4$ at different temperatures.

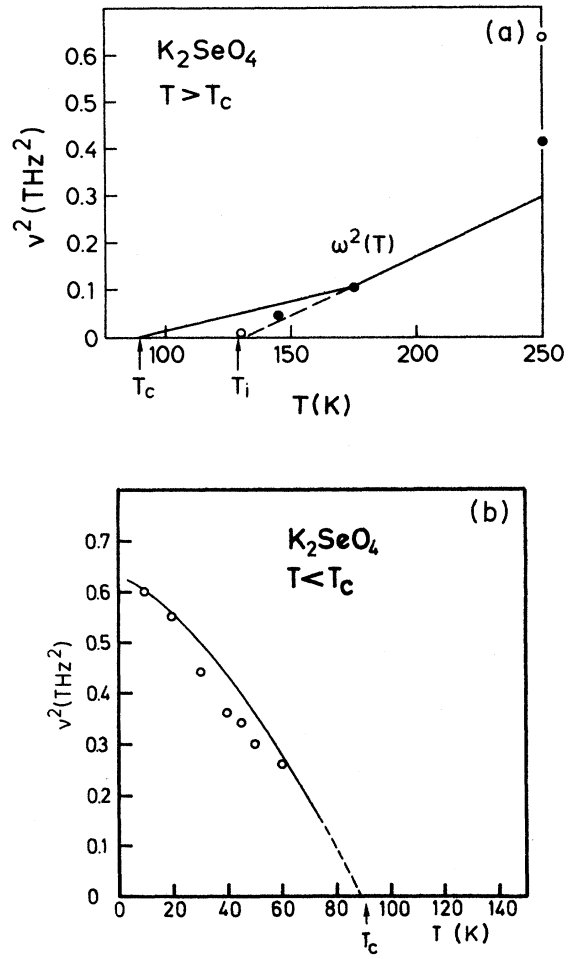


FIG. 10. Comparison of experimental (Ref. 37) (circles) and theoretical temperature dependences of $\omega_F^2$ in (a) the paralectric and incommensurate phases of $K_2SeO_4$, and (b) the ferroelectric phase of $K_2SeO_4$.

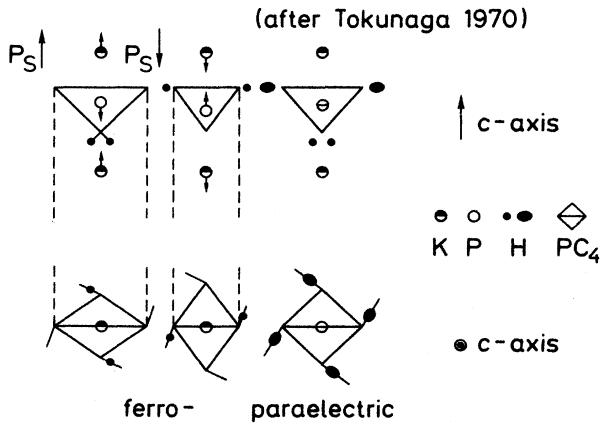


FIG. 11. Schematic structure of $KH_2PO_4$ in the ferroelectric and the paraelectric state, in accordance with Ref. 42.

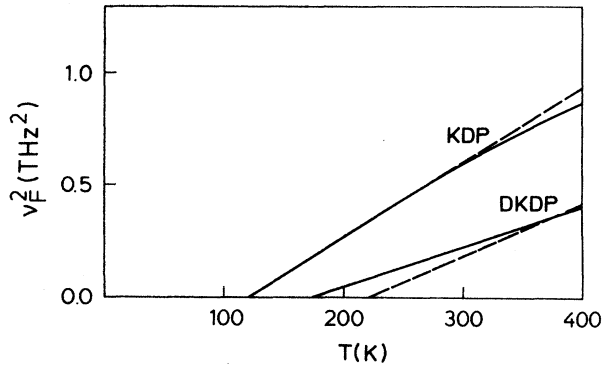


FIG. 12. Comparison of experimental (Ref. 46) (dashed lines) and theoretical (solid lines) temperature dependences of $\omega_F^2$ for $KH_2PO_4$ (KPD) and $KD_2PO_4$ (DKDP).

lographic direction, i.e., the $c$ axis, develops a spontaneous polarization at $T_c$. Simultaneously, the protons order in the perpendicular $a,b$ plane without showing a macroscopic dipole moment (Fig. 11).[43,44] For these compounds the polarizability model was extended by including the local double-well potential of the protons in the calculations.[45] Thus, the second mass $m_2$ now represents the protonic mass, and its core-shell force constants account for this nonlinear potential by including attractive harmonic forces $g_2^{(2)}$ and repulsive stabilizing forces $g_4^{(2)}$. Now, the original mode represents a coupled double-well problem where both fourth-order terms are treated in the self-consistent phonon approximation, and thus require a double-self-consistent treatment which has been described in Ref. 45. The soft mode of KDP was calculated as a function of temperature, and is compared to experimental data[46] in Fig. 12. The replacement of hydrogen by deuterium shifts $T_c$ to higher values and simultaneous-

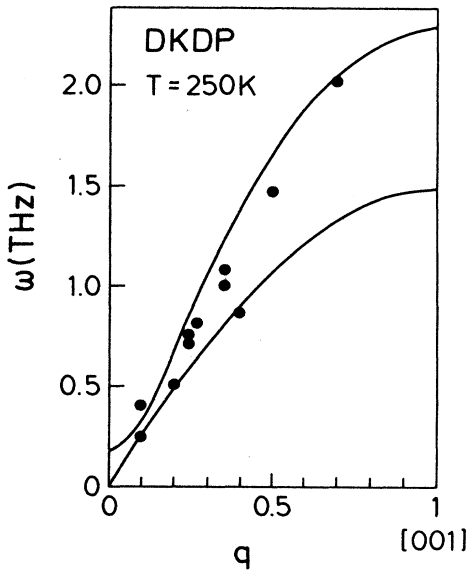


FIG. 13. Comparison of calculated dispersion curves (lines) with experimental data (Ref. 47) for DKDP at $T=250$ K.

ly induces a change in its Curie constant. All model parameters are unchanged, and as can be seen in Fig. 12, the agreement of theoretical and experimental data is fairly good. As inelastic neutron scattering data[47] are available for DKDP only, we compared the dispersion curves of this compound with the model calculations which is depicted in Fig. 13. Here, the agreement is nearly perfect.

Replacing K by Rb, Cs, or $NH_4$, or replacing $PO_4$ by $AsO_4$ experimentally, also results in a shift in $T_c$ which is, of course, less spectacular than the replacement of hydrogen by twice its mass. Yet, these replacements require a change in the phonon-phonon and electron-phonon interactions $f'_{(1)}, f$ to be reproduced by the model. The isotope effect on $T_c$ and the Curie constant in these isomorphic compounds is of the same order of magnitude as in KDP, and the model calculations reproduce the correct trend but are not in perfect agreement with experiment. A more refined treatment of hydrogen-bonded ferroelectrics is in progress and will be published in another paper.

## VI. ANTIFERROELECTRIC COMPOUNDS AND ITS MIXED CRYSTALS WITH FERROELECTRIC COMPOUNDS

Until now we concentrated on model calculations with repulsive intersite electron-phonon and phonon-phonon interactions, i.e., $f, f'_{(1)} > 0$. Stable solutions of the nonlinear model with lower energy are obtained for, e.g., $f<0, f'_{(1)}>0$ or $f>0, f'_{(1)}<0$ which, in the static limit, exhibit an antiferroelectric displacement pattern or superstructures with higher-order periods as, e.g., 3 or 4, etc.[48] The continuum limit even allows soliton or breather-type displacement patterns with lowest energy.[49]

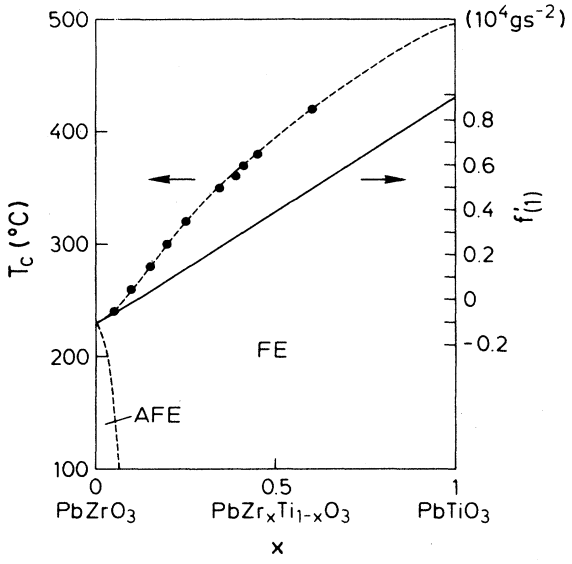


FIG. 14. Phase diagram of the transition temperature $T_c$ as a function of composition $x$ of $PbZr_{1-x}Ti_xO_3$ in accordance with Ref. 51, together with $x$-dependent intersite phonon-phonon coupling $f'_{(1)}$.

Here, we investigate the competition between ferroelectricity and antiferroelectricity as has been observed, for instance, in $PbTi_xZr_{1-x}O_3$.[50] The phase diagram[51] of the mixed crystals is depicted in Fig. 14. The lattice dynam-

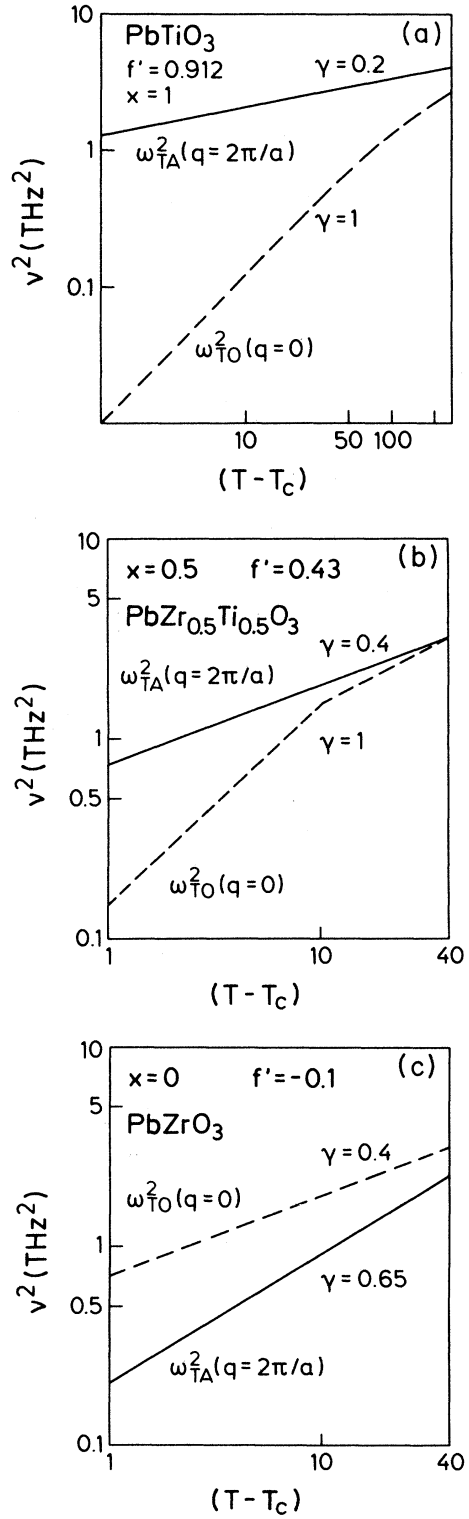


FIG. 15. Temperature dependences of $\omega_F^2$ and $\omega_{TA}^2$ $(q=2\pi/a)$ for (a) $PbTiO_3$, (b) $PbZr_{0.5}Ti_{0.5}O_3$ and (c) $PbZrO_3$.

ics of $PbTiO_3$ have been described in the first section. We investigated the mixed crystals by assuming that the phonon-phonon interaction $f'_{(1)}$ scales linearly with the phase transition temperature $T_c$ which is shown in the same figure. Thus, the mass $m_1$ and the intersite coupling $f'_{(1)}$ are a function of composition $x$. For the antiferroelectric compound $f'_{(1)}$ is attractive, leading to a softening of the acoustic zone-boundary frequency $\omega_{TA}$ $(q=2\pi/a)$ with decreasing $g(T)$. At $T_c$, $\omega_{TA}=0$, which involves a doubling of the lattice cell and, simultaneously, an antiferroelectric order. Also, $\omega^2_{TO}$ $(q=0)$ as well $\omega^2_{TA}$ $(q=2\pi/a)$ have been calculated as functions of temperature for different compositions $x$. Interestingly, the critical exponent of the soft optic mode of $PbTiO_3$ which is here in accordance with mean-field predictions changes to smaller values than 1 and exhibits a value of 0.4 in the antiferroelectric compound $PbZrO_3$. For the zone-boundary mode the reversed change in its critical exponent is observed. While in the ferroelectric compound, $PbTiO_3$, $\omega^2_{TA}$ $(q=2\pi/a)$ only displays a slight temperature dependence with a critical exponent $\gamma\cong 0.2$, its temperature dependence becomes steeper with increasing $x$ and exhibits at the antiferroelectric border a value of 0.65. The temperature dependence of both modes is shown in Figs. 15 for three different compositions $x=1$, 0.5, and 0.0. Experimental data are not available for the mixed crystals, and thus the model calculations are hopefully a challenge to experimentalists.

In conclusion, it has been shown that antiferroelectric transitions can also be described by the polarizability model and that a change in critical exponents $\gamma$ with composition $x$ is expected from the model calculations.

## CONCLUSIONS

We have shown that the polarizability model in its one-dimensional version describes qualitatively and quantitatively displacive-type ferroelectric phase transitions in structurally different ferroelectric compounds. The strong anisotropy of the development of a ferroelectric dipole moment allows the application of this model, as here only one axis is lattice dynamically relevant for the soft-mode behavior and related temperature-dependent quantities. The model parameters can be directly related to the phase transition temperature and their changes permit us to draw conclusions about the change in physical properties.

## ACKNOWLEDGMENTS

We thank H. Büttner and H. Vogt for useful discussions and a critical reading of the manuscript. One of us (G.B.) acknowledges the hospitality extended at the Max-Planck-Institut für Festkörperforschung, Stuttgart, where this work was accomplished. One of us (A.B.-H.) acknowledges the support of the Deutsche Forschungsgemeinschaft.

*Deceased.

[1]H. Bilz, G. Benedek, and A. Bussmann-Holder, Phys. Rev. B **35**, 4840 (1987).

[2]A. Bussmann-Holder, H. Bilz, R. Roenspiess, and K. Schwarz, Ferroelectrics **25**, 343 (1980).

[3]R. Migoni, H. Bilz, and D. Bäuerle, Phys. Rev. Lett. **37**, 1155 (1976).

[4]H. Bilz, A. Bussmann, G. Benedek, H. Büttner, and D. Strauch, Ferroelectrics **25**, 339 (1980).

[5]A. Bussmann-Holder, G. Benedek, H. Bilz, and B. Mokross, J. Phys. (Paris) Colloq. **6**, C6-409 (1981).

[6]B. Wul and I. M. Goldmann, C.R. (Dokl.) Acad. Sci. URSS **46**, 139 (1945); **49**, 177 (1945).

[7]B. T. Matthais, Phys. Rev. **75**, 1771 (1949).

[8]B. T. Matthais and J. P. Remeika, Phys. Rev. **76**, 1886 (1949).

[9]G. Shirane, S. Hoshino, and K. Suzuki, Phys. Rev. **80**, 1105 (1950).

[10]W. Cochran, Adv. Phys. **9**, 387 (1960).

[11]R. Comés and G. Shirane, Phys. Rev. B **5**, 1886 (1972); G. Shirane, R. Nethans, and V. G. Minkiewicz, Phys. Rev. **157**, 396 (1967); J. D. Axe, J. Harada, and G. Shirane, Phys. Rev. B **1**, 1227 (1970).

[12]R. A. Cowley, Phys. Rev. **134**, A981 (1964); W. G. Stirling and R. Currat, J. Phys. C **9**, L519 (1976); W. G. Stirling, *ibid.* **5**, 2711 (1972).

[13]G. Shirane, J. D. Axe, J. Harada, and J. P. Remeika, Phys. Rev. B **2**, 155 (1970).

[14]H. Bilz, H. Büttner, A. Bussmann-Holder, W. Kress, and U. Schröder, Phys. Rev. Lett. **48**, 264 (1982).

[15]T. Schneider, H. Beck, and E. Stoll, Phys. Rev. B **13**, 1123 (1976).

[16]See, e.g., for reviews Yu. I. Ravich, B. A. Efimova, and I. A. Smirnov, in *Semiconducting Lead Chalcogenides,* edited by L. S. Stil'bans (Plenum, New York, 1970); R. Dalven, Solid State Phys. **28**, 179 (1973); D. R. Lovett, in *Semimetals and Narrow-Bandgap Semiconductors* (Pion Limited, London, 1977); L. Ley, M. Cardona, and R. A. Pollak, in *Photoemission in Solids* (Springer, Berlin, 1979), Vol. II.

[17]H. Kawamura, in *Physics of Narrow-Gap Semiconductors,* edited by J. Rautuszkiewicz, M. Gorska, and E. Kaamarek (Elsevier, New York, 1977); K. Murase, J. Phys. Soc. Jpn. Suppl. **49**, 727 (1980); S. Katayama and D. L. Mills, Phys. Rev. B **22**, 336 (1980); K. Schubert and H. Fricke, Z. Naturforsch. **6a**, 781 (1951); E. F. Steigmeier and G. Harbeke, Solid State Commun. **8**, 1275 (1970).

[18]R. A. Cowley, Philos. Mag. **11**, 673 (1965); J. Goldak, C. S. Berett, D. Imes, and W. Youdelis, J. Chem. Phys. **44**, 3323 (1966); D. K. Hohnke, H. Holloway, and S. Kaiser, J. Phys. Chem. Solids **33**, 2053 (1972).

[19]T. Chattopadhyay, A. Werner, and H. G. v. Schnering, Rev. Appl. Phys. **19**, 807 (1984).

[20]A. Bussmann-Holder, H. Bilz, and P. Vogl, in *Electronic and Dynamical Properties of IV-VI Compounds,* Vol. 99 of *Springer Tracts in Modern Physics,* edited by G. Höhler (Springer, Berlin, 1983).

[21]M. M. Elcombe, Proc. R. Soc. London **A300**, 210 (1967).

[22]P. R. Vijayaraghavan, S. K. Sinha, and P. K. Iyengar (unpublished).

[23]W. Cochran, R. A. Cowley, G. Dolling, and M. M. Elcombe, Proc. R. Soc. London **A293**, 433 (1966).

[24]R. A. Cowley, J. K. Darby, and G. S. Pawley, J. Phys. C **2**, 1916 (1969).
[25]A. Bussmann-Holder, W. Kress, H. Bilz, and U. Schröder, in *Proceedings of the International Conference on the Physics of Narrow Gap Semiconductors, Linz, 1981,* edited by E. Gornick, H. Henrich and L. Palmetshofer (Springer, Berlin, 1982).
[26]H. A. Alperin, S. J. Pickardt, J. J. Rhyne, and V. J. Minkiewicz, Phys. Lett. **40A**, 295 (1972).
[27]K. Murase and S. Sugai, Solid State Commun. **32**, 89 (1979).
[28]E. Dönges, Z. Anorg. Chem. **263**, 112 (1950); **265**, 56 (1951).
[29]M. Balkanski, M. K. Teng, M. Massot, and H. Bilz, Ferroelectrics **26**, 737 (1980).
[30]E. Fatuzzo, G. Harbeke, W. J. Merz, R. Nitsche, H. Roetschi, and W. Ruppel, Phys. Rev. **127**, 2036 (1962).
[31]R. Nitsche, H. Roetschi, and P. Wild, Appl. Phys. Lett. **4**, 210 (1964); T. A. Pikka and V. M. Fridkin, Fiz. Tverd. Tela **10**, 3378 (1968).
[32]M. Massot, thesis, Paris, 1986 (unpublished).
[33]J. P. Pouget, S. M. Shapiro, and K. Nassau, J. Phys. Chem. Solids **40**, 267 (1979).
[34]D. K. Agrawal and C. H. Perry, Phys. Rev. B **4**, 1893 (1971).
[35]A. Aika, K. Hukuda, and O. Matumura, J. Phys. Soc. Jpn. **26**, 1064 (1969).
[36]K. Aika and K. Hukuda, J. Phys. Soc. Jpn. **26**, 1066 (1969).
[37]M. Iizumi, J. D. Axe, G. Shirane, and K. Shimaoka, Phys. Rev. B **15**, 4392 (1977).
[38]A. Kalman, J. S. Stephens, and D. W. J. Cruickshank, Acta Crystallogr. B **26**, 1451 (1970).
[39]W. Bantle, Helv. Phys. Acta **15**, 373 (1942).
[40]R. Blinc and B. Zeks, J. Phys. C **15**, 4661 (1982); Y. Takagi, J. Phys. Soc. Jpn. **3**, 271 (1984).
[41]M. Ichikawa, Acta Crystallogra. Sect. B **34**, 2074 (1978); M. Tokunaga and J. Tatsuzaki, Phase Trans. **4**, 37 (1984); M. Ichikawa, K. Motida, and N. Yamada, Phys. Rev. B **36**, 874 (1978).
[42]T. Matsubara, Jpn. J. Appl. Phys. **24-2**, 1 (1985).
[43]G. E. Bacon and R. S. Pease, Proc. R. Soc. London Ser. A: **220**, 397 (1953); **230**, 359 (1955).
[44]M. Tokunaga, Ferroelectrics **1**, 195 (1970).
[45]A. Bussmann-Holder and H. Bilz, Ferroelectrics **54**, 5 (1984); A. Bussmann-Holder and H. Büttner, *ibid.* **80**, 297 (1988).
[46]Y. Takagi, Ferroelectrics **46**, 245 (1983).
[47]J. Skalyo, B. C. Frazer, and G. Shirane, Phys. Rev. B **1**, 278 (1970).
[48]H. Büttner and H. Bilz, Adv. Solid State Phys. **23**, 13 (1983).
[49]G. Benedek, A. Bussmann-Holder, and H. Bilz, Phys. Rev. B **36**, 630 (1987).
[50]E. Sawaguchi and T. Kittaka, J. Phys. Soc. Jpn. **7**, 336 (1952).
[51]G. Shirane and S. Hoshino, J. Phys. Soc. Jpn. **6**, 265 (1951); E. Sawaguchi, G. Shirane, and Y. Takagi, *ibid.* **6**, 333 (1951); S. Roberts, J. Am. Ceram. Soc. **33**, 63 (1950).